

Brake Detection for Electric Bicycles using Inertial Measurement Units

Jan Schnee, Jürgen Stegmaier, Tobias Lipowsky
Robert Bosch GmbH
Gerlingen-Schillerhöhe, Germany
Jan.Schnee@de.bosch.com

Pu Li
Process Optimization Group
Institute for Automation and Systems Engineering
Ilmenau University of Technology, Ilmenau, Germany
Pu.Li@tu-ilmenau.de

Abstract—The traffic situation of today's streets is changing through an increase in light electrical vehicular transportation systems. One of those systems is the electronically power assisted cycle (EPAC). As this vehicle group is regarded as strongly exposed, the improvement of cycling safety and the analysis of the rider-behavior is gaining importance. By integrating inertial measurement based brake detection systems, both goals are simultaneously addressed. The approach presented in this paper estimates the brake magnitude of electric bicycles by combining the state-of-the-art brake detection methods and a model-based longitudinal dynamics system to achieve not only a fast response time, but also a reliable detection of persistent braking situations. The experimental results show good accuracy and the influence of further pre-estimated parameters is evaluated through a sensitivity analysis.

Keywords—electric bicycle, MEMS, brake detection, mass estimation

I. INTRODUCTION

To improve the rider-safety, a brake detection for electric bicycles enables various possibilities. For instance, a brake light can enhance the visibility for other road-users in critical situations. Another potential use case is reflecting the braking behavior to the user, so that bad or aggressive braking habits can be reduced by training instructions. In addition, it is possible to set up an overall rider analysis. The acquired knowledge is of high importance for bike manufacturers, traffic psychology and further more. In the automotive sector, insurance companies already started to offer reduced insurance rates for less aggressive drivers monitored by cameras [1]. This could be extended to inertial measurement unit (IMU) based driving style analysis approaches.

The state-of-the-art brake detection systems are either based on a switch on the braking lever (e.g. in the motorcycle use-case [2]) or on an acceleration sensor approach. Such acceleration sensor based systems use simple thresholding methods based on longitudinal vehicle acceleration signals, allowing only to detect aggressive or harsh braking. Further disadvantages of such methods are presented in section III [3], [4].

In this paper, we present a brake detection and brake intensity estimation of electric bicycles by using an IMU, an atmospheric pressure sensor and a longitudinal bike dynamics model. This system is able to detect harsh braking situations as well as continuous soft downhill braking scenarios. Furthermore, the application of the proposed approach in test scenarios shows an improved accuracy and sensitivity in comparison to the existing approaches.

II. BASICS

This section provides basics and the state-of-the-art approaches necessary for developing a new braking estimation method.

A. Calibration of the IMU

The IMU delivers the sensor data in the sensor frame coordinate system. One requirement for bike state estimation like a brake detection is the availability of sensor data in the vehicle / bike frame coordinate system (BF). Therefore, the sensor data has to be calibrated or transformed regarding the mounting orientation on the electric bicycle. As sensor errors of consumer IMUs are relative large [5], a second calibration addressing the sensor biases has to be implemented. The method in [6] uses bike-specific motions to calibrate both significant influencing factors. The benefit of this approach is its low amount of computations, the possibility to run it online, as well as not requiring special movements or known environmental parameters. For improved sensor bias estimations, an additional atmospheric pressure sensor is set up.

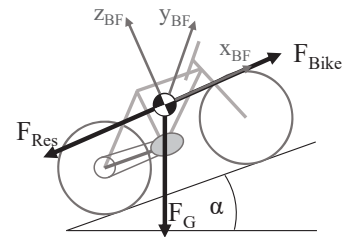


Fig 1. Representation of longitudinal dynamics and vehicle frame system BF (bike frame)

B. Attitude Estimation

The goal of fusing the sensor data of the accelerometer and the gyroscope is to have an estimation of the pitch angle of the bicycle. The advantage of the sensor fusion lies in a more independent estimation of short acceleration periods such as drive-off and deceleration processes. A reliable pitch estimation is mandatory for the longitudinal dynamics model.

The fusion filter used here is a complementary filter by Sebastian Madgwick [7]. It is based on quaternions and relies on a gradient descent algorithm of the accelerometer component, combined with a simple integration of the rotational rates of the gyroscopes. Therefore, it is computationally inexpensive and shows satisfactory results in attitude estimation.

C. Bike Longitudinal Dynamics Model

To determine the operating state of a bike, e.g. if a bike is accelerated or decelerated, an overall force F_{Bike} and the driving resistance F_{Res} of the longitudinal dynamics model [8] is required. In Fig. 1 the relation between driving resistances F_{Res} and its environment is shown. The relation of these resistances can be described as [9]:

$$F_{Res} = F_{air} + F_{roll} - F_{slope} + F_{inertia} \quad (1)$$

The air resistance F_{air} is a flow resistance composed of the air volume in front of the bike-rider-system which is being moved and the friction of the air:

$$F_{air} = \frac{\rho_{air}}{2} * c_d * A * v_{flow}^2 \quad (2)$$

Typical values of the front surface A of the bike-rider-system ranges between 0.4-0.5 m² and of the aerodynamic drag coefficient c_d between 0.83-1.02 [10]. ρ_{air} is the density of the air and v_{flow} is the sum of the bike speed ($v_{Bike} = \dot{x}_{Bike}$) and the wind speed.

The roll resistance F_{roll} is the product of the weight force and the rolling friction coefficient μ_r (0.00160 - 0.00696 [11]) and the factor x_U (1 - 3, [8]), which corresponds to the different sub-surfaces [8].

$$F_{roll} = m_{system} * g * \mu_r * x_U * \cos(\alpha) \quad (3)$$

The slope resistance F_{slope} is the downhill force:

$$F_{slope} = m_{system} * g * \sin(\alpha) \quad (4)$$

The last but important resistance of the longitudinal dynamics model is the inertia resistance $F_{inertia}$. It affiliates to the inertia force of the system and it is composed of the linear acceleration of the overall system and the rotation of the wheels [8]. Both components depend on the bike acceleration a_{Bike} and the rotational part of the inertia torque θ_{wheels} (~0.4kgm², [8]; r_{wheel} corresponds to the radius of the wheels of the bicycle):

$$F_{inertia} = a_{Bike} * \left(m_{system} + \frac{\theta_{wheels}}{r_{wheel}^2} \right) \quad (5)$$

III. METHOD

A. Analyzing Bike Braking

A bicycle is decelerating if F_{res} is greater than the accelerating force F_{Bike} introduced by the motor and/or by the rider itself (see Fig. 1). A deceleration of the bicycle does not have to be necessarily caused by the rider, for instance if it is caused by an increasing slope. On the other hand, the rider can be braking even without decelerating, i.e. without reducing the speed, especially when riding downhill.

Due to the fact that our approach aims to trigger only in proper braking scenarios where the rider is actually pulling the braking lever, it is not possible just to use a simple acceleration threshold as described in [3] and [4]. These methods would cause many false positives as well as false negatives.

In the following, the two braking cases (with and without reducing the speed) will be further analyzed and algorithms for the detection will be introduced.

B. Detecting short-term and harsh braking scenarios

The braking intervention which actually leads to a reduction of speed is here defined as a short-term and harsh braking (STHB). Such scenarios are emergency stops or caused by unexpected occurrences. Furthermore people with a fast, sportive and/or aggressive riding behavior show such braking scenarios, too.

As already mentioned, the methods proposed in [3], [4] address such braking scenarios by comparing the acceleration in driving direction with a threshold (-0.11 and -0.12 g in [3]). One disadvantage of these methods is shown with the following example: If a cautious rider is driving with 18 km/h and takes 5 s for constant deceleration until standing in front of the traffic light, then the bike will be decelerating with -0.1 g and cannot be detected by such approaches.

For detecting the STHB, we take the measured and low pass filtered acceleration in the driving direction $a_{x,filt}$ and the estimated pitch angle α of the sensor fusion algorithm, to compensate the gravity component in the driving direction. The derived deceleration value a_{STHB} is one input for our combined brake detection algorithm and is similar to the state-of-the-art methods in [3] and [4].

$$a_{STHB} = a_{x,filt} + \sin(\alpha) \quad (6)$$

The advantage of accelerometer/IMU based approaches is the independence of the time delay of the commonly used speed signals like reed-sensors which sample only one time per rotation in electric bicycle applications. One disadvantage is the complete inability to detect braking interventions of the rider without any speed loss.

C. Detecting long-term persistent braking scenarios

It is possible to ride a bike downhill and pulling the brake lever, but still not reducing - maybe even increasing - the speed, due to the downhill force. In these cases, the longitudinal dynamics model of the bicycle (LDM) is combined with Newton's second law:

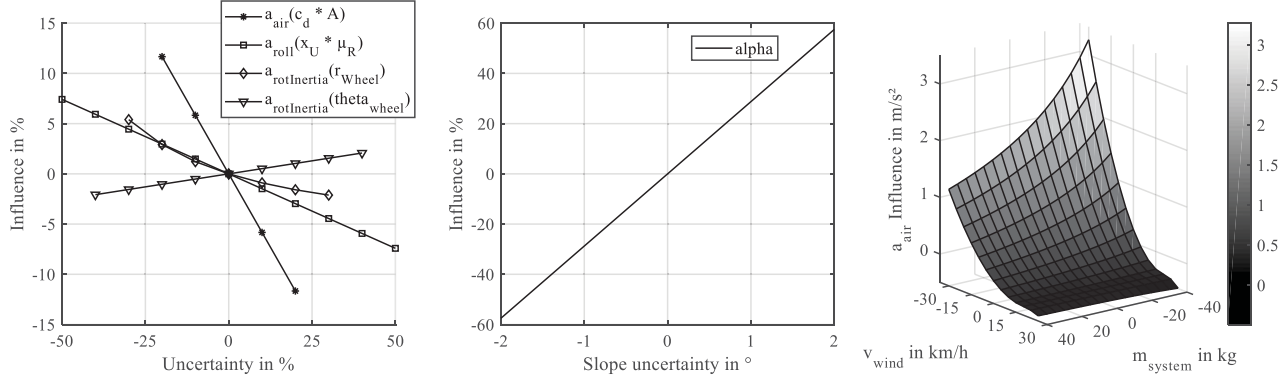


Fig 2. Results of SA (operating point: $v_{Bike} = 20 \text{ km/h}$, slope = 0° , deceleration = -1 m/s^2 , $m_{system} = 100 \text{ kg}$); I shows relative dependence of several model parameters; II represents the influence on the accuracy of the slope estimation of the calibrated IMU; III exhibits the strong influence of wind effects and imprecise mass estimations.

$$F_{Res} = F_{Bike} = m_{system} * a_{LDM} \quad (7)$$

$$a_{LDM} = \frac{F_{Res}}{m_{system}} = \frac{F_{air} + F_{roll} - F_{slope} + F_{inertia}}{m_{system}} \quad (8)$$

$$a_{LDM} = \frac{\frac{\rho_{air}}{2} * c_d * A * v_{flow}^2}{m_{system}} + g * \mu_r * x_U * \cos(\alpha) - g * \sin(\alpha) + a_{Bike} * \left(1 + \frac{\Theta_{wheels}}{r_{wheel}^2 * m_{system}}\right) \quad (9)$$

If the acceleration a_{LDM} is below zero, the bike experiences a further resistance (F_{Bike}), which might but not necessarily has to lead to a loss of speed. This part of the deceleration is only caused by the braking intervention of the user. All other causes are theoretically considered in the other four resistances of the LDM (see Eq. (1)).

The disadvantage of this approach is its complexity and the variety of parameters. As already mentioned, the time delay of the speed signal leads to a time delay of the acceleration signal a_{Bike} , which can be expressed as the time derivation of v_{Bike} ($a_{Bike} = \frac{dv_{Bike}}{dt} = \frac{d\dot{x}_{Bike}}{dt} = \ddot{x}_{Bike}$). But this variable delay becomes smaller with higher speed values, due to the increasing amount of wheel rotations, i.e. more sensor triggers per time period.

D. Parameter Sensitivity and System Mass Estimation

The influence of this parameter set ($c_d, A, \mu_r, x_U, \Theta_{wheels}, r_{wheel}, m_{system}$) of the LDM has to be analyzed. This sensitivity analysis (SA) will identify the parameters affecting the model's accuracy of the LDM. Each SA is only valid for one scenario, and thus one representative operating point has to be defined. After the SA for one operating point (OP), conclusions regarding the general influence onto the system can be made. The chosen OP represents a standard braking phase: the speed is at 20 km/h on an even horizontal surface ($\alpha = 0^\circ$) and the rider starts to reduce the speed with -1 m/s^2 . In this setting, there is no wind and the system mass is set as 100 kg. This standard parameter set is defined from the mean literature values and is varied according to the ranges described in [8], [10], [11]. The influence of the wind speed and the system mass is analyzed separately. At this OP, the deceleration caused by the braking intervention is calculated as

-0.88 m/s^2 , the delta of -0.12 m/s^2 is used as a result by the other driving resistances.

The results of the SA are shown in Fig 2. The first plot (I) confirms the minor influence of several model parameters on the brake detection estimation. Especially the rotational inertia $a_{rotInertia}$ and roll component a_{roll} and its presented model parameter demonstrate this behavior. The air resistance exposes a slightly greater influence of 11 % at 20 % uncertainty of the drag coefficient at the operating point. The second plot (II) shows another part of the SA and demonstrates the importance of an accurate slope estimation: here, an error of 1° causes even an error of 28.8 % (linear relation) of the deceleration estimation caused by the brake intervention. Therefore, the benefit of the slope is its signal characteristics which should be online calibrated and fused. But the necessity of an accurately real-time calibration and sensor fusion remains.

The most challenging parameters are the system mass as well as the wind speed which has to be set for estimating the air friction. In the third plot (III) of Fig 2, the correlation between the air friction and the system mass in relation to the wind speed is outlined. The influence of the system mass changes relatively to the wind speed. If there is no wind speed, the accuracy of the brake intensity estimation will be sufficient with an input accuracy of the mass of $\pm 15 \text{ kg}$. On the basis of these results, it can be determined that a braking intervention detection with headwinds above 15 km/h is impossible. In this case, the influence of the wind on to the bike dynamics is so extensive that the rider interventions cannot be distinguished anymore. Unfortunately, the wind speed cannot be estimated separately with the current setup. Therefore, it has to be ignored, despite its huge influence during high wind speed events.

The above derived knowledge of the SA will be used for the threshold design.

E. System mass estimation

The system mass can be estimated online by evaluating specific riding scenarios with respect to the LDM. Existing event-based approaches for the automotive use case usually evaluate scenarios with specific acceleration changes [12],

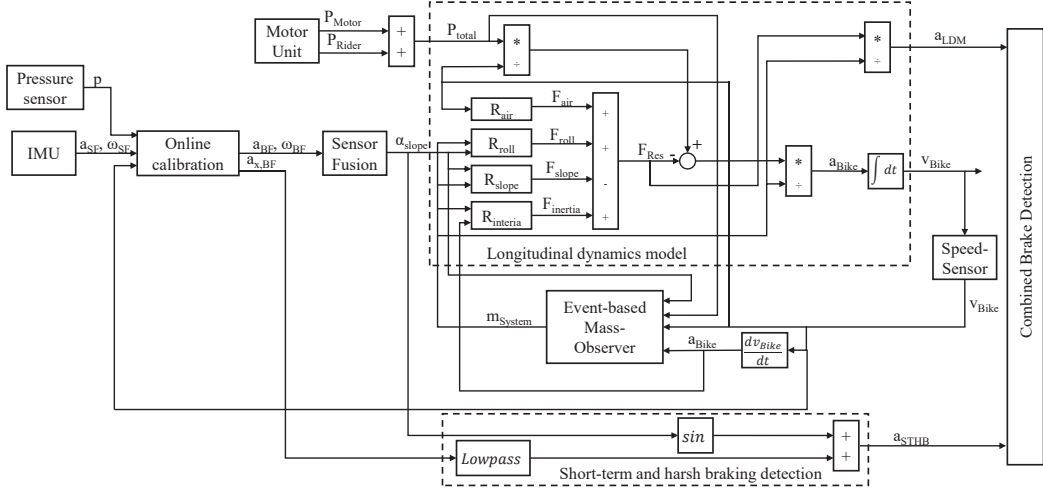


Fig 3. Flow chart of complete system.

[13]. Those riding scenarios are considered, such that the mass has the greatest influence on all driving resistances in relation to the other model parameters. For the specific electric bicycle use case, those scenarios are driving-off/acceleration and uphill phases.

First, the system equation (1) has to be set up regarding to the powering force F_{Bike} :

$$F_{Bike} = F_{Res} = F_{air} + F_{roll} - F_{slope} + F_{inertia} \quad (10)$$

$$F_{Bike} = \frac{P_{total}}{v_{Bike}} = \frac{P_{Bike} + P_{Rider}}{v_{Bike}} \quad (11)$$

The necessary powers (P_{Bike} and P_{Rider}) are measured signals of the motor unit of the electric bicycle – the sum of these powers represents P_{total} . Subsequently, the equation can be solved for the system mass parameter m_{system} :

$$m_{System} = \frac{\frac{P_{total}}{v_{Bike}} - \frac{\rho_{air} * c_d * A * v^2}{2} * \sin(\alpha)}{-g * \sin(\alpha) + g * \mu_r * x_U * \cos(\alpha) + a_{Bike}} \quad (12)$$

In section VI the functionality of the mass estimation is going to be analyzed.

F. Combined System

The signal flow with all components of the proposed approach is presented schematically in Fig. 3. The IMU data undergoes a calibration by analyzing the speed and pressure data. The calibrated accelerations and rotational rates in the vehicle coordinate system are used for the sensor fusion. Afterwards, the STHB and the LDM model for the brake detection as well as the brake intensity estimation follow. The mass estimation is implemented as an event-based observer using (12).

Using this framework, each estimation method (STHB and LDM) can activate the brake intervention trigger by itself, even though the STHB approach can not directly estimate the brake intensity of the interaction of the rider. The a_{LDM} threshold is based on the gained knowledge of the SA and set as -0.5 m/s^2 . This allows a certain model parameter variance, but should still detect most of the common bike braking cases. For a_{STHB} a greater threshold of -0.8 m/s^2 is chosen due to its non-holistic

consideration of the overall model. It represents 2/3 of the automotive study value of [3]. For both methods the slope estimation shows the greatest relevance of all parameters. The third component of the brake detection is the combination of the STHB and the LDM approach. This combination is realized as 40 % of both thresholds, which are linked by a logic “and”.

Consequently, the proposed method makes use of the advantages of both mechanisms. Harsh braking interventions are detected fast, meanwhile continuous braking interventions with low or even no speed losses are not dismissed. Furthermore, a lot of the second types of braking scenarios start with a small jerk at the beginning. Here, the STHB guarantees a quick and first detection and the LDM takes over the task afterwards.

IV. EXPERIMENTAL RESULTS

The setup of the test bike is a standard electric trekking bicycle. As a reference for the brake state detection, brake pressure sensors for both brakes were set up. The ground truth deceleration intensity remains unknown, nevertheless a qualitative assessment via the brake pressure and the current speed should give a good hint about the estimated deceleration intensity. The ground truth for the mass estimation is measured offline by industrial scales.

A. Mass Estimation

Tests for both events with good characteristics regarding mass estimation (acceleration and uphill passages) were carried out for evaluating the accuracy of the model regarding the mass estimation as well as the model validation. The results are presented in Fig.4 (driving-off scenarios) and Fig.5 (uphill scenario). Caused by the characteristic of persisting uphill scenarios, these driving states have a better convergence behavior and a higher accuracy. The reason for this is that alternating input signals (e.g. rider power) lead to a lower error influence over long evaluation periods. After 25 s of the test ride, acceptable convergence ($\sim 104.7 \text{ kg}$, ground truth: 103.4 kg) occurred, whereas the driving-off phases take several event repetitions to achieve useful results. After four

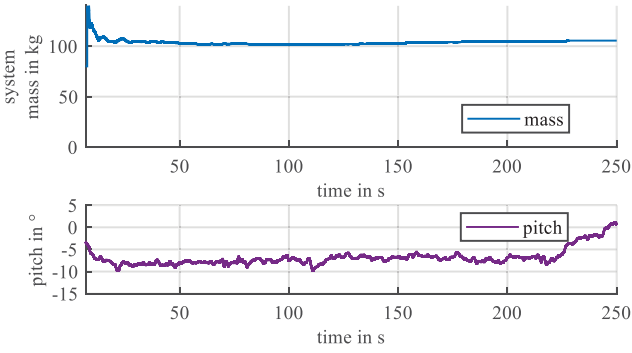


Fig 5. System mass estimation results during uphill scenario; ground truth = 103.4 kg, estimated mass alternates between 101.2 kg and 105.5 kg after a point in time of 20 s

acceleration procedures the mass estimation returns a system mass of 99.4 kg (ground truth: 108.0 kg).

Both evaluations show acceptable results of the system mass regarding the brake detection and brake intensity estimation. The defined range, by the SA of ± 15 kg, is maintained. Nevertheless, the frequency of occurrence of the necessary driving states is strongly dependent on the bike user and its environment.

The influence of the wind shows a similar behavior as in the results described in the previous section. I.e. high wind speeds will degrade the functionality of the mass estimation. During the presented test rides, there was no wind. Due to the lack of detecting wind with the current bike setup, its influence was neglected. Furthermore, the influence of special bicycle models like fat-bikes are not part of this evaluation.

B. Brake Detection and Brake Intensity Estimation

The brake detection and brake intensity estimation were tested in both braking cases to verify both approaches and to show the advantages of the combined system. The plotted deceleration curves represent the deceleration caused by the braking intervention. The total deceleration of the

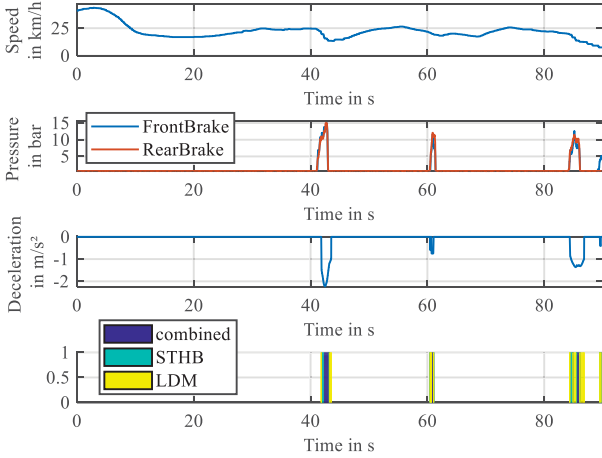


Fig 6. Brake detection and brake intensity estimation results; fast detection of the STHB approach, followed by delayed combined and LDM approach;

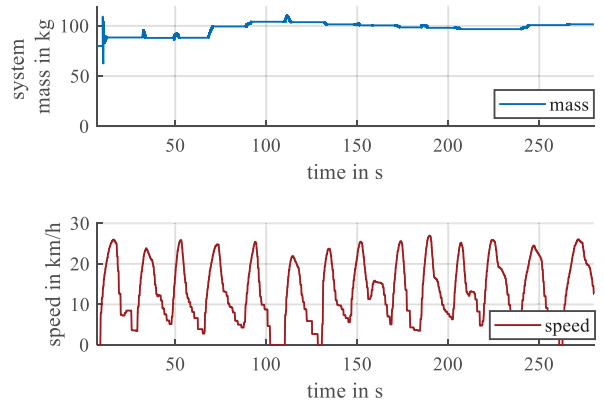


Fig 4. System mass estimation results during 14 driving-off scenarios; ground truth = 108.0 kg, estimated mass alternates between 99.4 kg and 103.7 kg after already four acceleration phases

rider-bicycle-system is a supplementary combination of the other presented driving resistances. During the test rides there was no strong (head-) wind.

In Fig. 6, normal braking scenarios (e.g. before traffic lights or turns) occurred. The first braking takes place shortly after 40 s and shows the quick response of the STHB approach, due to the high deceleration value of up to -2 m/s^2 . With a small delay the LDM method triggers as well, which leads to a following combined estimation. At the end, the last braking has a similar characteristic - only the smaller speed loss leads to a further part of this braking case, which can be detected only by the single LDM approach. The second braking has only a small deceleration intensity ($\sim 0.7 \text{ m/s}^2$) and is therefore not detected by the single STHB threshold. Since the methods in [3] and [4] use the similar approaches to our STHB method, they would not detect these braking situations either.

Fig. 7 shows a long-term persistent braking scenario. The downhill passage starts at the time of 45 s and exhibits a slope of up to 13 % ($\sim 7.5^\circ$). In the time between 70 s and 90 s the

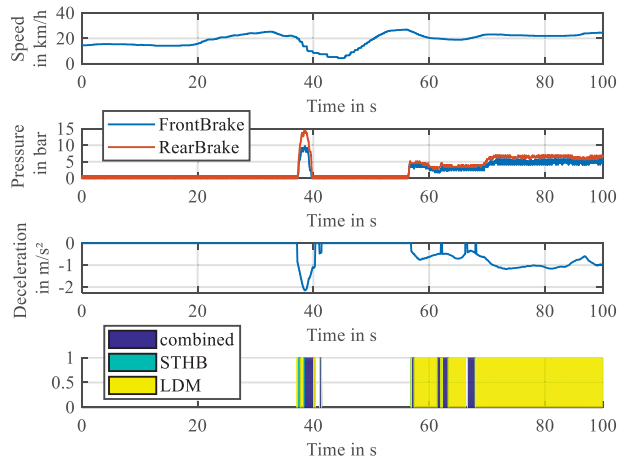


Fig 7. Brake detection and brake intensity estimation during a downhill scenario; the speed is not changing despite prevailing brake pressure on both brakes (due to the downhill force); braking scenario is still being detected by the LDM method;

speed remains constant, despite the applied braking pressure. Therefore, the STHB is completely unable to detect a braking intervention, but the LDM triggers. Between 60 s and 70 s three short false negative estimations occurred, caused by the small braking intervention of the rider. Nevertheless, the threshold set shows good functionality over all test rides. Some observed situations with high accelerations/decelerations combined with high dynamic turning interactions could lead to an imprecise slope fusion. Associated with the analyzed strong influence of the slope parameter, this result confirms the threshold setting, too.

The deceleration intensity estimations show in all cases good correlation to the braking pressure, while considering the current speed. Furthermore, the high quality of the results can be taken as a validation of the setup model and the selected parameters.

V. CONCLUSION

We presented a model based brake detection approach for electric bicycles. The longitudinal bike dynamics model is used for detecting brake interventions and brake intensity of the user in combination with a simple longitudinal acceleration based approach. A sensitivity analysis showed the influence of all model parameters for a specific braking use case and is used as the base for the threshold design.

In addition, the setup combination for detecting braking interventions of the bicycle rider and estimating the braking intensity showed good results in experimental test rides. Our approach is able to detect braking situation having only 50 % of the magnitude of the state-of-the-art methods. Thus, it is more sensitive and is able to detect more braking cases and scenarios. The system designed in this way is ready to use for analyzing different riders and their riding behaviors.

REFERENCES

- [1] Sunday Times Driving, "<https://www.driving.co.uk/>," 17 August 2018. [Online]. Available: <https://www.driving.co.uk/car-clinic/best-car-insurance-discounts-dash-cam-users/>.
- [2] Economic Comission for Europe of the United Nations, "ACTS ADOPTED BY BODIES CREATED BY INTERNATIONAL AGREEMENTS - Regulation No 7 (UN/ECE)," *Official Journal of the European Union*, p. 2, 2014.
- [3] P. Mohan, V. N. Padmanabhan and R. Ramjee, "Nericell: rich monitoring of road and traffic conditions using mobile smartphones," *Proceedings of the 6th ACM conference on Embedded network sensor systems*, pp. 323-336, 2008.
- [4] D. A. Johnson and M. M. Trivedi, "Driving style recognition using a smartphone as a sensor platform," *2011, 14th International IEEE Conference on Intelligent Transportation Systems (ITSC)*, pp. 1609-1615, 2011.
- [5] "BMI160 - Datasheet Small, low power inertial measurement unit," 2015.
- [6] J. Schnee, J. Stegmaier and P. Li, "Auto-Calibration of Bias Compensated 2D-Mounting Orientation of an IMU on an Electric Bicycle using Bike-Specific Motions," *InProceedings of 2018 IEEE SENSORS*, pp. 1440-1443, 2018.
- [7] S. Madgwick, "An efficient orientation filter for inertial and inertial/magnetic sensor arrays," *Report x-io and University of Bristol (UK)*, vol. 25, pp. 113-118, 2010.
- [8] M. Gressmann, *Bicycle physics and biomechanics [Fahrradphysik und Biomechanik: Technik, Formeln, Gesetze]* pp. 38-56, Bielefeld: Moby Dick, 2010.
- [9] J. Kühlwein, "Driving Resistances of Light-Duty Vehicles in Europe: Present Situation, Trends, and Scenarios for 2025," *The international council on clean transportation*, vol. 49, pp. 1-4, 2016.
- [10] H. Chowdhury and F. Alam, "Bicycle aerodynamics: an experimental evaluation methodology," *Sports Engineering*, vol. 15, pp. 73-80, 2012.
- [11] T. Senkel, "Plea for a good tyre [Plädoyer für einen guten Reifen]," *ProVelo* 32, 1993.
- [12] M. Breen, "System and method for determining relative vehicle mass". US Patent 5482359, 1 1996.
- [13] J.-H. Montonen and T. Lindh, "Event-seeking Mass Estimator for Hybrid Working Machine," *13th International Symposium" Topical Problems in the Field of Electrical and Power Engineering". Paernu, Estonia, 14-18 Jan. 2013*, pp. 147-149, 2013.